AD-A052 231 ARMY ELECTRONICS COMMAND FORT MONMOUTH N J F/G 20/5
INVESTIGATION OF ABRUPT DECREASES IN ATMOSPHERICALLY BACKSCATTE--ETC(U)
DEC 77 R RUBIO

UNCLASSIFIED ECOM-5835 NL

| OF |
AD
A052 231

END
DATE
FILMED
5-78
DDC

AD

Reports Control Symbol
OSD-1366

RESEARCH AND DEVELOPMENT TECHNICAL REPORT

ECOM-5835

INVESTIGATION OF ABRUPT DECREASES IN ATMOSPHERICALLY BACKSCATTERED LASER ENERGY

By

Robert Rubio

1L161102B53A

Atmospheric Sciences Laboratory
US Army Electronics Command
White Sands Missile Range, New Mexico 88002

29 P.

Dec 77

Approved for public release; distribution unlimited.

ECOM

UNITED STATES ARMY ELECTRONICS COMMAND - FORT MONMOUTH, NEW JERSEY 07703

037 620

NOTICES

Disclaimers

The findings in this report are not to be construed as an official Department of the Army position, unless so designated by other authorized documents.

The citation of trade names and names of manufacturers in this report is not to be construed as official Government indorsement or approval of commercial products or services referenced herein.

Disposition

Destroy this report when it is no longer needed. Do not return it to the originator.

SECURITY CLASSIFICATION OF THIS PAGE (When Data Entered)

REPORT DOCUMENTATION PAGE

READ INSTRUCTIONS BEFORE COMPLETING FORM

1. REPORT NUMBER: ECOM-5835
2. GOVT ACCESSION NO.:
3. RECIPIENT'S CATALOG NUMBER:
4. TITLE (and Subtitle): INVESTIGATION OF ABRUPT DECREASES IN ATMOSPHERICALLY BACKSCATTERED LASER ENERGY
5. TYPE OF REPORT & PERIOD COVERED: R&D Technical Report
6. PERFORMING ORG. REPORT NUMBER:
7. AUTHOR(s): Robert Rubio
8. CONTRACT OR GRANT NUMBER(s):
9. PERFORMING ORGANIZATION NAME AND ADDRESS: Atmospheric Sciences Laboratory, White Sands Missile Range, New Mexico 88002
10. PROGRAM ELEMENT, PROJECT, TASK AREA & WORK UNIT NUMBERS: DA Task No. 1L161102 B53A
11. CONTROLLING OFFICE NAME AND ADDRESS: US Army Electronics Command, Fort Monmouth, New Jersey 07703
12. REPORT DATE: December 1977
13. NUMBER OF PAGES: 22
14. MONITORING AGENCY NAME & ADDRESS (if different from Controlling Office):
15. SECURITY CLASS. (of this report): UNCLASSIFIED
15a. DECLASSIFICATION/DOWNGRADING SCHEDULE:
16. DISTRIBUTION STATEMENT (of this Report): Approved for public release; distribution unlimited.
17. DISTRIBUTION STATEMENT (of the abstract entered in Block 20, if different from Report):
18. SUPPLEMENTARY NOTES:
19. KEY WORDS (Continue on reverse side if necessary and identify by block number):
Aerosols
Temperature inversion
Lidar
20. ABSTRACT (Continue on reverse side if necessary and identify by block number):

The objective of this study was to determine if two abrupt decreases, as a function of altitude, in atmospherically backscattered laser energy were directly associated with temperature inversion particulate trapping. A ruby lidar system was employed to detect the sharp decreases in laser energy at altitudes of 2.22 km and 2.56 km on the night of 1 November 1974. Aerosols of radius $r < 0.1\mu m$ and $1 < r < 3\mu m$, collected onboard the da Vinci balloon gondola on the same night provided aerosol density versus altitude profiles. Temperature

next page

DD FORM 1 JAN 73 1473 EDITION OF 1 NOV 65 IS OBSOLETE

micrometers

SECURITY CLASSIFICATION OF THIS PAGE (When Data Entered)

20. ABSTRACT (cont)

and relative humidity altitude profiles, recorded with radiosonde instruments at 2045, 1 November, and 0415, 2 November, revealed the absence of temperature inversions within the laser probed altitude interval. Abrupt changes in relative humidity failed to induce similar changes in the reflected laser energy. The sharp decreases in backscattered laser energy are attributed to a negative density gradient of the 1 μm to 3 μm radius anhydrous aerosols. This gradient was not located above a temperature inversion and therefore, in this case, the changes in laser signal were found to be unrelated to any temperature inversion trapping mechanism.

micrometers

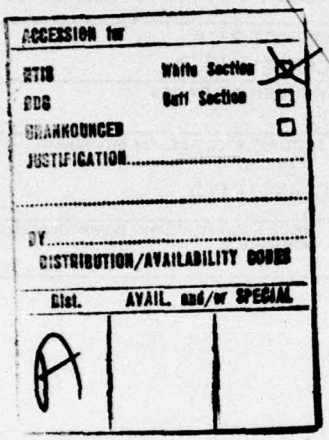

CONTENTS

INTRODUCTION

The results reported here are part of the overall experiment entitled "Project da Vinci" which was conducted on 1 and 2 November 1974. The Chief of the Research Division, RDE Directorate, Army Materiel Command issued the directive that the Atmospheric Sciences Laboratory actively participate and partially fund Project da Vinci. Consequently, the experiment described herein was carried out, as were other experiments, in response to that directive.

Laser detection and ranging systems (lidar) have been shown to have the potential for detecting subsidence temperature inversions which have formed in the atmosphere [1]. Early lidar detection of temperature inversion formations can serve as an additional source of information which can contribute to making weather forecasting more effective; however, the inversion lidar "signatures" are still not sufficiently defined for prognostication purposes. Since each inversion signature is actually caused by laser energy reflections from trapped particulates, additional concurrently sampled aerosol concentrations, atmospheric temperature structure, and backscattered laser energy data are needed. Project da Vinci, a manned balloon flight, instrumented to obtain comprehensive meteorological samples and measure aerosol concentrations, and scheduled to float in the vicinity of the ground based lidar to be described below, afforded an excellent opportunity to acquire the aforementioned concurrent data samples. Thus the objective of the lidar experiment described here was to obtain laser energy atmospheric reflections as a function of altitude which, in conjunction with the da Vinci in situ aerosol data and the accompanying radiosonde data, would further assist in clarifying the lidar's temperature inversion signature characteristics.

Lidar probing was conducted from Small Missile Range, White Sands Missile Range, New Mexico. The balloon trajectory was in a generally northeastern direction from Las Cruces, New Mexico (2045, 1 November 1974), to Wagon Mound, New Mexico (0830, 2 November 1974). This path brought the balloon aerosol sensors within 20 km of the lidar. Temperature and relative humidity versus altitude profiles were acquired with standard radiosonde instruments released at 2045, 1 November, and 0415, 2 November, in the proximity of the da Vinci balloon path. This report briefly describes the lidar system, the fundamental laser energy backscattering equation, and laser atmospheric data collected during Project da Vinci. It identifies two inversion-type lidar signatures and investigates aerosol density, temperature, and relative humidity versus altitude profiles to determine the mechanism which produced the lidar inversion-type signatures.

GB-60B LIDAR SYSTEM

The Sandia Laboratory GB-60B lidar system (Fig. 1) was employed during Project da Vinci. This system consists primarily of a "Q-switched" ruby laser transmitter, a Cassegrainian telescope, light filter, and a photomultiplier comprising the receiver, an ME-16 tracking mount with sighting

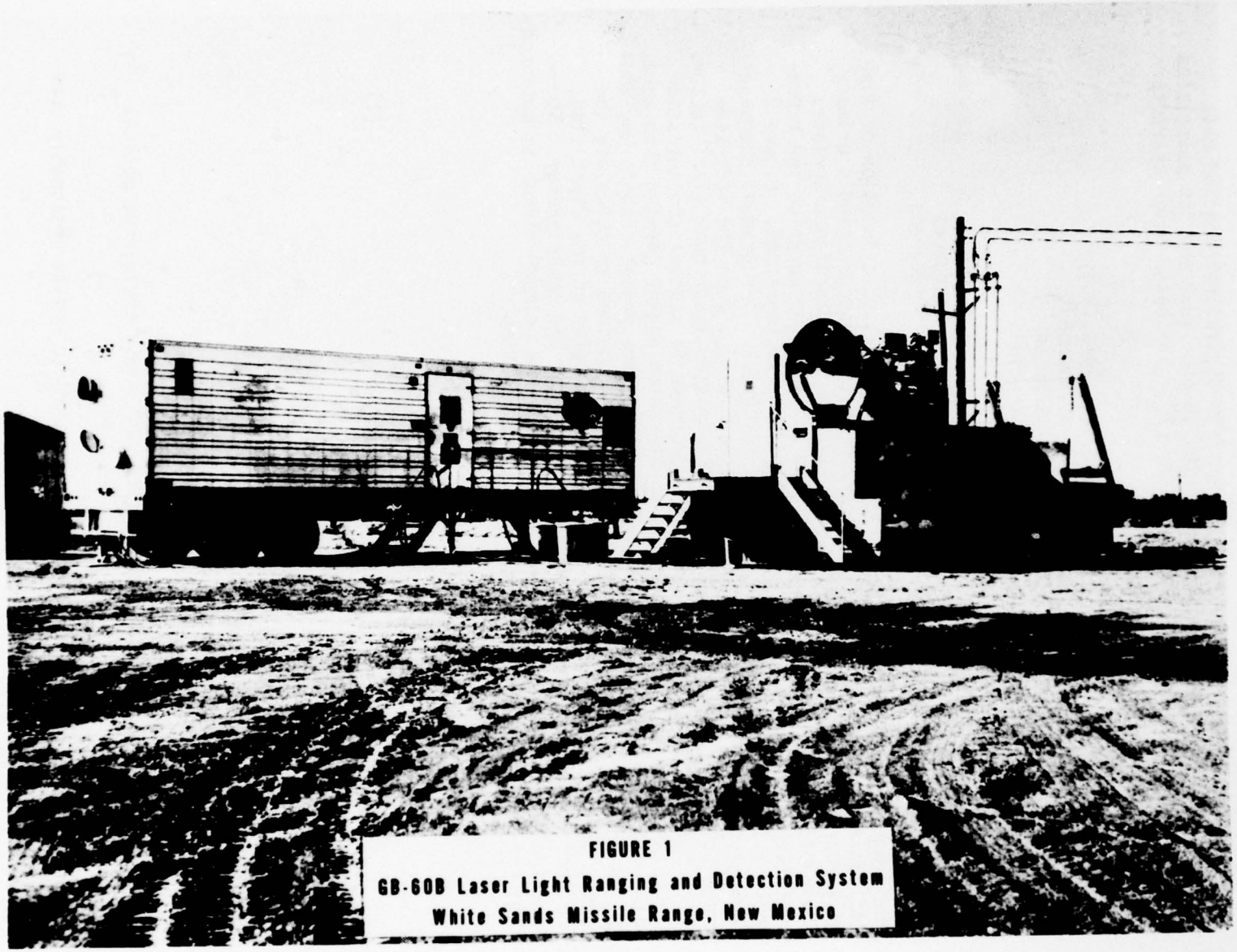

FIGURE 1

GB-60B Laser Light Ranging and Detection System
White Sands Missile Range, New Mexico

telescopes, and the electronic equipment for digital ranging and data recording. A detailed description of the GB-60B lidar and its associated equipment is given by Landry and Lockner [2]. The basic laser characteristics are:

Wavelength	6943 angstroms (Ruby)
Pulse width	20-35 nanoseconds
Maximum output energy	4 joules/pulse
Maximum beam divergence	85 milliradians
Photomultiplier	RCA 7265-S20
Receiver aperture	1.68 M^2
Sighting capability	Azimuth 0 to 360 degrees Elevation 0 to 90 degrees

The lidar's oscilloscope records voltage amplitudes as a function of time. Reflected laser light energy is collected by the Cassegrainian's primary mirror and is focused onto the photomultiplier's photocathode surface. The photomultiplier output is fed to the oscilloscope on which the representative voltage amplitudes are displayed and photographed. Figure 2 shows a typical laser atmospheric data photograph. The gradual decrease in amplitude with increasing height as seen in Fig. 2 on the left side trace is due to the divergence of the transmitted laser beam ($1/r^2$ factor, where r is the slant range) and to the decrease in scatter concentration since the lidar is usually pointing at elevation angles greater than zero. Time gating of the oscilloscope photograph and the preset scope's horizontal sweep time provide the timing information required to calculate the target slant ranges. Figure 2 also displays a pulse on the right side. The area within this pulse provides a measure of the laser energy. Atmospherically reflected light power incident on the primary mirror is obtained from the recorded voltages by employing the relation

$$P_i = \frac{v}{gR_iR_\lambda N_o}, \qquad (1)$$

where

v = voltage
g = photomultiplier gain
R_i = oscilloscope input impedance
R_λ = photomultiplier responsivity
N_o = product of mirrors, light filter, and glass enclosures optical efficiencies

The parameters g, R_i, R_λ, and N_o may be assumed to remain reasonably contant during the lasing period of one mission.

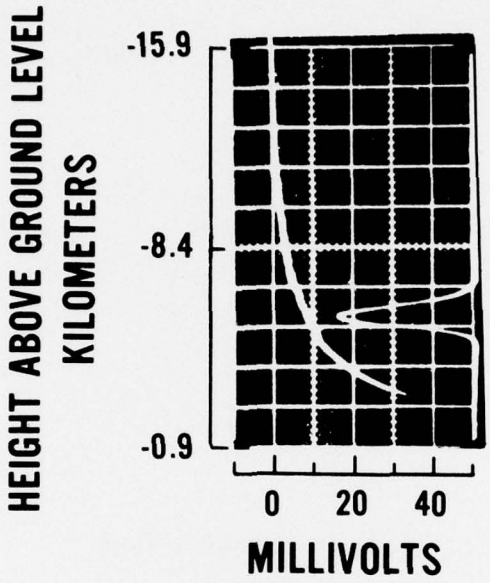

FIGURE 2. LEFT TRACE: VOLTAGE AMPLITUDES, WHICH ARE PROPORTIONAL TO ATMOSPHERICALLY BACKSCATTERED LASER LIGHT ENERGY, AS A FUNCTION OF HEIGHT. RIGHT SIDE PULSE IS A MEASURE REPRESENTATIVE OF LASER OUTPUT ENERGY.

BASIC LIDAR THEORY

In the coaxial arrangement of the lidar's transmitter and receiver, the fraction of the atmospherically backscattered light power which is collected by the primary mirror is given, with sufficient accuracy for the present purposes, by the relation

$$P_i = \frac{P_t c \tau A}{8\pi r^2} \beta(r) \exp\left[-2 \int_0^r \alpha(r)dr\right], \tag{2}$$

where

P_i = light power incident on primary mirror
P_t = transmitted power
c = the velocity of light
τ = pulse width
A = receiver aperture
r = range
$\beta = \beta_m(r) + \beta_a(r)$
β_m = molecular volume backscattering coefficient
β_a = aerosol volume backscattering coefficient
$\alpha = \alpha_m(r) + \alpha_a(r)$
α_m = molecular extinction coefficient
α_a = aerosol extinction coefficient

The volume backscattering coefficient β is equal to the product of the backscattering cross-sectional area (m^2) of the specific particle and the particle number density (m^{-3}).

Elimination of the power quantity P_i in Eq. 2 with the use of Eq. 1 yields the expression

$$v = \frac{KP_t\tau}{r^2} \left[\beta_a(r) + \beta_m(r)\right] \exp\left[-2 \int_0^r \alpha dr\right], \tag{3}$$

where

$$K = \frac{gR_i R_\lambda N_o c A}{8\pi}. \tag{4}$$

Equation 3 demonstrates that the lidar's oscilloscope voltage deflections (to be presented as data later) are, through the β parameter, proportional to aerosol and molecular concentrations. Within the first 4 km of the atmosphere the aerosol volume backscattering coefficient, at ruby wavelengths, exceeds the molecular backscattering coefficient by factors of 1.5 to 10 [3]. Consequently, in this altitude interval, the voltage amplitudes are more representative of aerosol densities and their variations than molecular density or its variations.

DATA RESULTS

Atmospherically backscattered laser energy data were recorded during the da Vinci balloon passage on 1 November 1974 from 1800 to 2100 MST. Although the altitudes probed ranged from 1.3 to 18.0 km MSL, only the laser data at altitudes which coincide with balloon heights at which in situ aerosol data were obtained are discussed here. The balloon reached a maximum altitude of 3.85 km MSL. The sequence of lidar photographs (Figs. 3, 4a, 4b) in which altitude overlaps from one photograph to the next shows voltage data (on the left side trace) as a function of altitude. These voltage profiles, recorded at 2045 MST, are representative of the general atmospheric light energy backscattering conditions which prevailed throughout the 3-hour lasing period.

Examination of Fig. 3 shows two abrupt decreases in backscattered laser energy at approximately 2.22 and 2.56 km. These abrupt decreases are typical of temperature inversion lidar signatures. The acute laser signal decreases occurred within an altitude interval of 100 m. Abrupt optical signal decreases such as these have been observed before and were associated with sharp reductions in aerosol concentrations above the temperature inversion [1]. During past lidar experiments, this author has observed similar optical signal decreases with respect to increasing altitude occurring concurrently with decreases of relative humidity immediately above the temperature inversion height. It has been suggested that the rapid changes in backscattered signal in this case are caused by an abatement of humid atmospheric layers containing hygroscopic nuclei which have grown through condensation processes [4]. The relatively smooth profiles in Figs. 4a and 4b indicate that between the voltage drop at 2.56 km and the balloon's maximum altitude, the atmosphere was characterized by an absence of anhydrous particulate concentrations or humid layers. Backscattered laser energy profiles similar to Figs. 4a and 4b have been reported to be representative of an atmosphere in which the aerosols are more uniformly distributed and are predominantly Aitken size continental particles [5].

Under the auspices of Dr. A. J. Alkezweeny of Pacific Northwest Laboratories (PNL) and Dr. R. F. Pueschel of the National Oceanic and Atmospheric Administration (NOAA), in situ aerosol concentration measurements were made from the balloon gondola with a Royco Model 220 Optical Sensor and a Gardner Small Particle Detector. The sampling systems were such that total concentrations recorded as a function of altitude were divided into particle

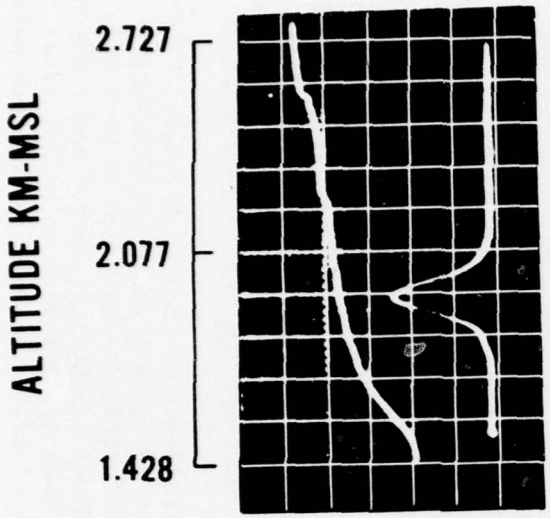

FIGURE 3

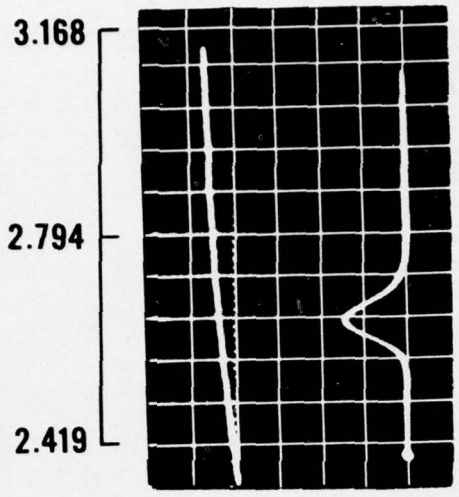

FIGURE 4a

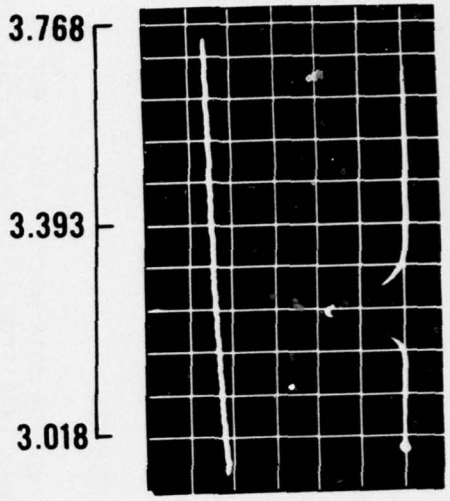

FIGURE 4b

LEFT TRACES: LIDAR RECORDED VOLTAGE AMPLITUDES AS A FUNCTION OF ALTITUDE. PROFILES DEPICT THE PREVAILING ATMOSPHERIC BACKSCATTERING CONDITIONS DURING PROJECT DA VINCI.

groups with diameter, d, less than 1/10μm (Aitken nuclei) and with radii ranging from 0.3μm to 3μm. At the GB-60B laser light wavelength of 0.69μm, the concentration variation of particles with radii > 0.1μm induces the larger backscattered signal fluctuations, provided the < 0.1μm aerosol densities are not excessive. Based on the NOAA data on total concentration of particles of radius $r \leq 0.1\mu m$, the backscattered energy due to aerosols of $r \leq 0.1\mu m$ was established to be less than that due to molecular scattering. Also particles of this size range will not have grown through condensation processes because the radius of curvature is below the critical size for which vapor and water droplet pressure are likely to exist in equilibrium. Accordingly, only aerosol data of radii group $0.3\mu m < r < 3\mu m$ was examined. In the latter group of data, the electronic pulses representative of aerosols in the radius group, $0.3\mu m \leq r < 1\mu m$, became embedded in the electronic noise and the data were not recovered. Consequently, only concentrations of particulates in the 1μm to 3μm radius group measured with PNL instrumentation were used for comparison with backscattered laser energy profiles.

Aerosol concentrations of the 1μm to 3μm radius size which were sampled between approximately 2300 and 2400 MST within the altitude region 2.28 to 3.84 km are plotted as a function of altitude in Fig. 5. Examination of Fig. 5 reveals the existence of a sharp decrease in aerosol concentrations from 2.2 to 2.8 km, a small increase from 2.8 to 3.1 km, and a more gradual decrease from 3.1 to 3.8 km. Comparison of Fig. 5 with the backscattered energy trace of Fig. 3 shows that the two abrupt drops in reflected laser energy at 2.22 and 2.56 km, which are typical of lidar inversion signatures, occurred within this altitude region where the aerosol density diminished from 1.2×10^6 to 3.4×10^5 particles/m^3. There was, unfortunately, a scarcity of data samples from 2 to 2.8 km which precluded designating the exact aerosol density gradient required of particles this size to induce such laser energy decreases. Nevertheless, it may be inferred that the sharp decreases in backscattered energy are due to a decrease in aerosol concentrations. A review of Figs. 4a and 4b clearly shows that the slight enhancement, 3.4×10^5 to 4.5×10^5 particles/m^3, and the succeeding decrease, 4.5×10^5 to 1.2×10^5 particles/m^3, in aerosol densities were not detected with the lidar system.

To determine whether temperature inversions or humid layers existed during the lasing period, atmospheric temperature and relative humidity data recorded with two standard radiosondes released at 2045 MST, 1 November 1974, and 0415 MST, 2 November 1974 were collected and are shown plotted in Fig. 6. These profiles illustrate the general temperature and water moisture conditions which prevailed during the intervening time period. This period includes those times within which laser atmospheric probing was conducted and the time at which the balloon aerosol sensors passed within 20 km of the GB-60B lidar probing sector, 2100 MST.

Inspection of Fig. 6 reveals that from an altitude of approximately 1.5 km, which is where the laser data commences, atmospheric temperatures followed a relatively consistent lapse rate of about 8.2°C/km up to at least an

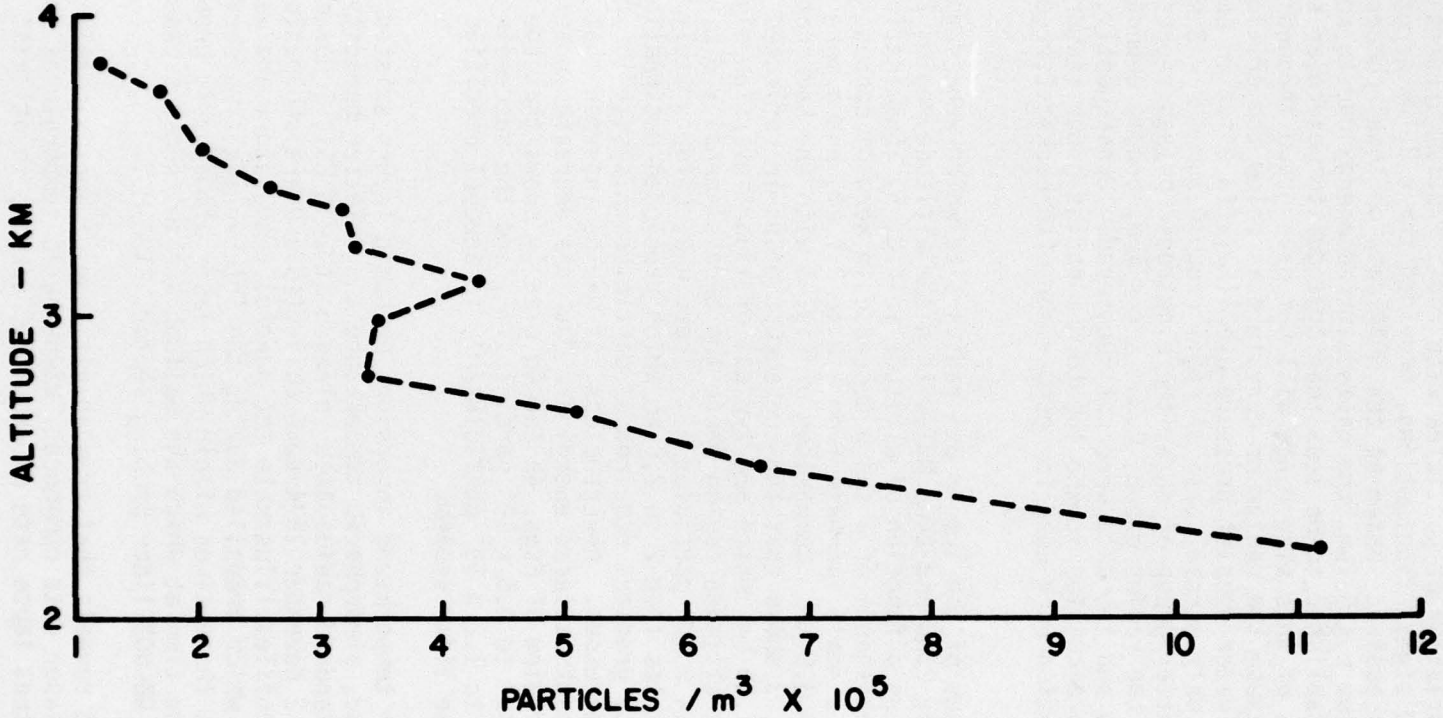

FIG. 5 AVERAGE AEROSOL CONCENTRATION FOR RADIUS; $1 < r < 3$ MICRON, PARTICLES COLLECTED DURING PROJECT DA VINCI FROM BALLOON GONDOLA WHILE OVER WSMR, N.M. 1 NOV 1974.

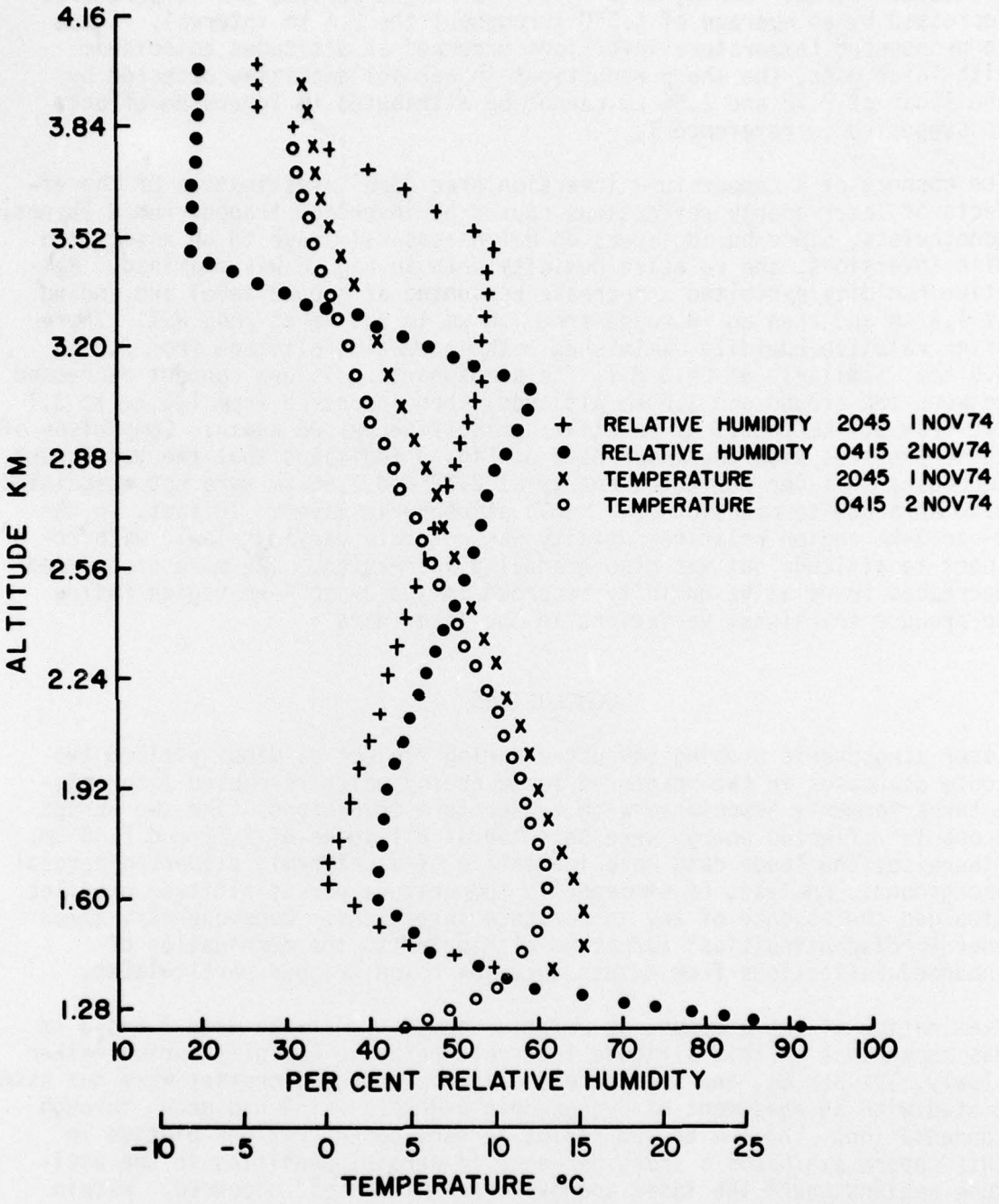

FIG. 6 RADIOSONDE RECORDED TEMPERATURE AND RELATIVE HUMIDITY AS A FUNCTION OF ALTITUDE FOR THE NIGHT OF NOV 1 - NOV 2, 1974.

altitude of 4 km. During this 7-1/2-hour night period, the temperatures decreased by an average of 1.5°C throughout the 2.5 km interval. Since no pronounced temperature inversions occurred at altitudes coincident with laser data, the sharp reductions in aerosol densities detected by the lidar at 2.22 and 2.56 km cannot be attributed to inversion effects as suggested in reference 1.

The absence of a temperature inversion precluded investigation of the effects of laser energy reflections caused by inversion trapped humid layers. Nonetheless, since humid layers do not necessarily have to be associated with inversions, the relative humidity data in Fig. 6 was examined. Relative humidity exhibited a decrease beginning at ground level and ending at 1.6 km and then an increase from 1.6 km to 3.5 km at 2045 MST. Thereafter relative humidity diminished with increasing altitude from 3.5 to 3.9 km. Similarly at 0415 MST, the atmospheric moisture content decreased between the ground and 1.6 km altitude, then increased from 1.6 km to 3.1 km; from 3.1 km to 3.5 km relative humidity decreased again. Comparison of these profiles with the laser data of Fig. 3 indicates that the two abrupt decreases in laser reflected energy at 2.22 and 2.56 km were not associated with an acute termination of a humid atmospheric layer. In fact, in the 2- to 3-km region relative humidity was not only varying slowly with respect to altitude but was also gradually increasing. The more pronounced decreases in relative humidity recorded in the 3- to 4-km region failed to produce any signal variations in the laser data.

CONCLUSIONS

Laser atmospheric probing conducted during Project da Vinci yielded two acute decreases in backscattered laser energy which resembled lidar signatures formerly associated with temperature inversions. The two abrupt drops in reflected energy were detected at altitudes of 2.22 and 2.56 km; otherwise, the laser data were indicative of a uniformly dispersed aerosol background. Analyses of atmospheric temperature versus altitude profiles divulged the absence of any temperature inversions. Consequently, these energy "discontinuities" cannot be attributed to the termination of enhanced reflections from temperature inversion trapped particulates.

Examination of the atmospheric relative humidity data between 2 and 3 km has shown that in this altitude interval, relative humidity varied rather slowly, 12% per km, and therefore the abrupt energy decreases were not associated with an abatement of hygroscopic aerosols which had grown through condensation. The 1μm to 3μm radius aerosol concentrations plotted in this report exhibited a sharp decrease in aerosol densities in the altitude regions where the laser energy "discontinuities" occurred. Within the same altitude interval, water moisture content was increasing. Therefore the laser data "discontinuities" are attributed to negative density gradients of anhydrous aerosols. More important, it has been shown that a lidar temperature inversion type signature can be induced by aerosol gradients without the mechanism of temperature inversion trapping.

Finally, based on the results of this experiment, and those relevant results in references 1 and 4, it is concluded that additional concurrent laser atmospheric probing, in situ aerosol measurements as a function of altitude, and radiosonde temperature and relative humidity measurements are required to identify the specific slope characteristics of laser energy discontinuities which may properly identify temperature inversions.

REFERENCES

1. Viezee, W., and J. Oblanas, 1969, "Lidar Observed Haze Layers Associated with Thermal Structure in the Lower Atmosphere," J. Appl. Meteorol., 8:369-375.

2. Laundry, M. J., and J. R. Lochner, 1968, "Laser Light Detecting and Ranging System GB-60A and GB-60B," Sandia Laboratories Report No. SC-DR-67-850.

3. McClatchey, R. A., R. W. Fenn, J. E. A. Selby, F. E. Voltz, and J. S. Garing, 1971, "Optical Properties of the Atmosphere," Air Force Cambridge Research Laboratories Report No. 71-0279.

4. Hamilton, P. M., 1966, "The Use of Lidar in Air Pollution Studies," Air Water Pollution Journal, 10.

5. Gambling, D. J., and K. Bartusek, 1972, "Lidar Observations of Tropospheric Aerosols," Atmospheric Environment, 6:181-190.

DISTRIBUTION LIST

Director
US Army Ballistic Research Laboratory
ATTN: DRDAR-BLB, Dr. G. E. Keller
Aberdeen Proving Ground, MD 21005

Air Force Weapons Laboratory
ATTN: Technical Library (SUL)
Kirtland AFB, NM 87117

Commander
Headquarters, Fort Huachuca
ATTN: Tech Ref Div
Fort Huachuca, AZ 85613

6585 TG/WE
Holloman AFB, NM 88330

Commandant
US Army Field Artillery School
ATTN: Morris Swett Tech Library
Fort Sill, OK 73503

Commandant
USAFAS
ATTN: ATSF-CD-MT (Mr. Farmer)
Fort Sill, OK 73503

Director
US Army Engr Waterways Exper Sta
ATTN: Library Branch
Vicksburg, MS 39180

Commander
US Army Electronics Command
ATTN: DRSEL-CT-S (Dr. Swingle)
Fort Monmouth, NJ 07703
03

CPT Hugh Albers, Exec Sec
Interdept Committee on Atmos Sci
Fed Council for Sci & Tech
National Sci Foundation
Washington, DC 20550

Inge Dirmhirn, Professor
Utah State University, UMC 48
Logan, UT 84322

HQDA (DAEN-RDM/Dr. De Percin)
Forrestal Bldg
Washington, DC 20314

Commander
US Army Aviation Center
ATTN: ATZQ-D-MA
Fort Rucker, AL 36362

CO, USA Foreign Sci & Tech Center
ATTN: DRXST-ISI
220 7th Street, NE
Charlottesville, VA 22901

Director
USAE Waterways Experiment Station
ATTN: Library
PO Box 631
Vicksburg, MS 39180

US Army Research Office
ATTN: DRXRO-IP
PO Box 12211
Research Triangle Park, NC 27709

Mr. William A. Main
USDA Forest Service
1407 S. Harrison Road
East Lansing, MI 48823

Library-R-51-Tech Reports
Environmental Research Labs
NOAA
Boulder, CO 80302

Commander
US Army Dugway Proving Ground
ATTN: MT-S
Dugway, UT 84022

HQ, ESD/DRI/S-22
Hanscom AFB
MA 01731

Head, Atmospheric Rsch Section
National Science Foundation
1800 G. Street, NW
Washington, DC 20550

Office, Asst Sec Army (R&D)
ATTN: Dep for Science & Tech
HQ, Department of the Army
Washington, DC 20310

Commander
US Army Satellite Comm Agc
ATTN: DRCPM-SC-3
Fort Monmouth, NJ 07703

Sylvania Elec Sys Western Div
ATTN: Technical Reports Library
PO Box 205
Mountain View, CA 94040

William Peterson
Research Association
Utah State University, UNC 48
Logan, UT 84322

Defense Communications Agency
Technical Library Center
Code 205
Washington, DC 20305

Dr. A. D. Belmont
Research Division
PO Box 1249
Control Data Corp
Minneapolis, MN 55440

Commander
US Army Electronics Command
ATTN: DRSEL-WL-D1
Fort Monmouth, NJ 07703

Commander
ATTN: DRSEL-VL-D
Fort Monmouth, NJ 07703

Meteorologist in Charge
Kwajalein Missile Range
PO Box 67
APO
San Francisco, CA 96555

The Library of Congress
ATTN: Exchange & Gift Div
Washington, DC 20540
2

US Army Liaison Office
MIT-Lincoln Lab, Library A-082
PO Box 73
Lexington, MA 02173

Dir National Security Agency
ATTN: TDL (C513)
Fort George G. Meade, MD 20755

Director, Systems R&D Service
Federal Aviation Administration
ATTN: ARD-54
2100 Second Street, SW
Washington, DC 20590

Commander
US Army Missile Command
ATTN: DRSMI-RRA, Bldg 7770
Redstone Arsenal, AL 35809

Dir of Dev & Engr
Defense Systems Div
ATTN: SAREA-DE-DDR
H. Tannenbaum
Edgewood Arsenal, APG, MD 21010

Naval Surface Weapons Center
Technical Library & Information
Services Division
White Oak, Silver Spring, MD
20910

Dr. Frank D. Eaton
PO Box 3038
Universtiy Station
Laramie, Wyoming 82071

Rome Air Development Center
ATTN: Documents Library
TILD (Bette Smith)
Griffiss Air Force Base, NY 13441

National Weather Service
National Meteorological Center
World Weather Bldg - 5200 Auth Rd
ATTN: Mr. Quiroz
Washington, DC 20233

USAFETAC/CB (Stop 825)
Scott AFB
IL 62225

Director
Defense Nuclear Agency
ATTN: Tech Library
Washington, DC 20305

Director
Development Center MCDEC
ATTN: Firepower Division
Quantico, VA 22134

Environmental Protection Agency
Meteorology Laboratory
Research Triangle Park, NC
27711

Commander
US Army Electronics Command
ATTN: DRSEL-GG-TD
Fort Monmouth, NJ 07703

Commander
US Army Ballistic Rsch Labs
ATTN: DRXBR-IB
APG, MD 21005

Dir, US Naval Research Lab
Code 5530
Washington, DC 20375

Mil Assistant for
Environmental Sciences
DAD (E & LS), 3D129
The Pentagon
Washington, DC 20301

The Environmental Rsch
Institute of MI
ATTN: IRIA Library
PO Box 618
Ann Arbor, MI 48107

Armament Dev & Test Center
ADTC (DLOSL)
Eglin AFB, Florida 32542

Range Commanders Council
ATTN: Mr. Hixon
PMTC Code 3252
Pacific Missile Test Center
Point Mugu, CA 93042

Commander
Eustis Directorate
US Army Air Mobility R&D Lab
ATTN: Technical Library
Fort Eustis, VA 23604

Commander
Frankford Arsenal
ATTN: SARFA-FCD-O, Bldg 201-2
Bridge & Tarcony Sts
Philadelphia, PA 19137

Director, Naval Oceanography and
Meteorology
National Space Technology Laboratories
Bay St Louis, MS 39529

Commander
US Army Electronics Command
ATTN: DRSEL-CT-S
Fort Monmouth, NJ 07703

Commander
USA Cold Regions Test Center
ATTN: STECR-OP-PM
APO Seattle 98733

Redstone Scientific Information Center
ATTN: DRDMI-TBD
US Army Missile Res & Dev Command
Redstone Arsenal, AL 35809

Commander
AFWL/WE
Kirtland AFB, NM 87117

Naval Surface Weapons Center
Code DT-22 (Ms. Greeley)
Dahlgren, VA 22448

Commander
Naval Ocean Systems Center
ATTN: Research Library
San Diego, CA 92152

Commander
US Army INSCOM
ATTN: IARDA-OS
Arlington Hall Station
Arlington, VA 22212

Commandant
US Army Field Artillery School
ATTN: ATSF-CF-R
Fort Sill, OK 73503

Commander and Director
US Army Engineer Topographic Labs
ETL-GS-AC
Fort Belvoir, VA 22060

Technical Processes Br-D823
NOAA, Lib & Info Serv Div
6009 Executive Blvd
Rockville, MD 20852

Commander
US Army Missile Research
and Development Command
ATTN: DRDMI-CGA, B. W. Fowler
Redstone Arsenal, AL 35809

Commanding Officer
US Army Armament Rsch & Dev Com
ATTN: DRDAR-TSS #59
Dover, NJ 07801

Air Force Cambridge Rsch Labs
ATTN: LCB (A. S. Carten, Jr.)
Hanscom AFB
Bedford, MA 01731

National Center for Atmos Res
NCAR Library
PO Box 3000
Boulder, CO 80307

Air Force Geophysics Laboratory
ATTN: LYD
Hanscom AFB
Bedford, MA 01731

Chief, Atmospheric Sciences Division
Code ES-81
NASA
Marshall Space Flight Center, AL 35812

Department of the Air Force
OL-C, 5WW
Fort Monroe, VA 23651

Commander
US Army Missile Rsch & Dev Com
ATTN: DRDMI-TR
Redstone Arsenal, AL 35809

Meteorology Laboratory
AFGL/LY
Hanscom AFB, MA 01731

Director CFD
US Army Field Artillery School
ATTN: Met Division
Fort Sill, OK 73503

Naval Weapons Center (Code 3173)
ATTN: Dr. A. Shlanta
China Lake, CA 93555

Director
Atmospheric Physics & Chem Lab
Code R31, NOAA
Department of Commerce
Boulder, CO 80302

Department of the Air Force
5 WW/DN
Langley AFB, VA 23665

Commander
US Army Intelligence Center and School
ATTN: ATSI-CD-MD
Fort Huachuca, AZ 85613

Dr. John L. Walsh
Code 4109
Navy Research Lab
Washington, DC 20375

Director
US Army Armament Rsch & Dev Com
Chemical Systems Laboratory
ATTN: DRDAR-CLJ-I
Aberdeen Proving Ground, MD 21010

R. B. Girardo
Bureau of Reclamation
E&R Center, Code 1220
Denver Federal Center, Bldg 67
Denver, CO 80225

Commander
US Army Missile Command
ATTN: DRDMI-TEM
Redstone Arsenal, AL 35809

Commander
US Army Tropic Test Center
ATTN: STETC-MO (Tech Library)
APO New York 09827

Commanding Officer
Naval Research Laboratory
Code 2627
Washington, DC 20375

Defense Documentation Center
ATTN: DDC-TCA
Cameron Station (Bldg 5)
Alexandria, Virginia 22314
12

Commander
US Army Test and Evaluation Command
ATTN: Technical Library
White Sands Missile Range, NM 88002

US Army Nuclear Agency
ATTN: MONA-WE
Fort Belvoir, VA 22060

Commander
US Army Proving Ground
ATTN: Technical Library
Bldg 2100
Yuma, AZ 85364

Office, Asst Sec Army (R&D)
ATTN: Dep for Science & Tech
HQ, Department of the Army
Washington, DC 20310

ATMOSPHERIC SCIENCES RESEARCH PAPERS

1. Lindberg, J.D., "An Improvement to a Method for Measuring the Absorption Coefficient of Atmospheric Dust and other Strongly Absorbing Powders, " ECOM-5565, July 1975.
2. Avara, Elton, P., "Mesoscale Wind Shears Derived from Thermal Winds," ECOM-5566, July 1975.
3. Gomez, Richard B., and Joseph H. Pierluissi, "Incomplete Gamma Function Approximation for King's Strong-Line Transmittance Model," ECOM-5567, July 1975.
4. Blanco, A.J., and B.F. Engebos, "Ballistic Wind Weighting Functions for Tank Projectiles," ECOM-5568, August 1975.
5. Taylor, Fredrick J., Jack Smith, and Thomas H. Pries, "Crosswind Measurements through Pattern Recognition Techniques," ECOM-5569, July 1975.
6. Walters, D.L., "Crosswind Weighting Functions for Direct-Fire Projectiles," ECOM-5570, August 1975.
7. Duncan, Louis D., "An Improved Algorithm for the Iterated Minimal Information Solution for Remote Sounding of Temperature," ECOM-5571, August 1975.
8. Robbiani, Raymond L., "Tactical Field Demonstration of Mobile Weather Radar Set AN/TPS-41 at Fort Rucker, Alabama," ECOM-5572, August 1975.
9. Miers, B., G. Blackman, D. Langer, and N. Lorimier, "Analysis of SMS/GOES Film Data," ECOM-5573, September 1975.
10. Manquero, Carlos, Louis Duncan, and Rufus Bruce, "An Indication from Satellite Measurements of Atmospheric CO2 Variability," ECOM-5574, September 1975.
11. Petracca, Carmine, and James D. Lindberg, "Installation and Operation of an Atmospheric Particulate Collector," ECOM-5575, September 1975.
12. Avara, Elton P., and George Alexander, "Empirical Investigation of Three Iterative Methods for Inverting the Radiative Transfer Equation," ECOM-5576, October 1975.
13. Alexander, George D., "A Digital Data Acquisition Interface for the SMS Direct Readout Ground Station — Concept and Preliminary Design," ECOM-5577, October 1975.
14. Cantor, Israel, "Enhancement of Point Source Thermal Radiation Under Clouds in a Nonattenuating Medium," ECOM-5578, October 1975.
15. Norton, Colburn, and Glenn Hoidale, "The Diurnal Variation of Mixing Height by Month over White Sands Missile Range, N.M," ECOM-5579, November 1975.
16. Avara, Elton P., "On the Spectrum Analysis of Binary Data," ECOM-5580, November 1975.
17. Taylor, Fredrick J., Thomas H. Pries, and Chao-Huan Huang, "Optimal Wind Velocity Estimation," ECOM-5581, December 1975.
18. Avara, Elton P., "Some Effects of Autocorrelated and Cross-Correlated Noise on the Analysis of Variance, " ECOM-5582, December 1975.
19. Gillespie, Patti S., R.L. Armstrong, and Kenneth O. White, "The Spectral Characteristics and Atmospheric CO2 Absorption of the Ho^{+3}:YLF Laser at 2.05μm," ECOM-5583, December 1975.
20. Novlan, David J. "An Empirical Method of Forecasting Thunderstorms for the White Sands Missile Range," ECOM-5584, February 1976.
21. Avara, Elton P., "Randomization Effects in Hypothesis Testing with Autocorrelated Noise," ECOM-5585, February 1976.
22. Watkins, Wendell R., "Improvements in Long Path Absorption Cell Measurement," ECOM-5586, March 1976.
23. Thomas, Joe, George D. Alexander, and Marvin Dubbin, "SATTEL — An Army Dedicated Meteorological Telemetry System," ECOM-5587. March 1976.
24. Kennedy, Bruce W., and Delbert Bynum, "Army User Test Program for the RDT&E-XM-75 Meteorological Rocket," ECOM-5588, April 1976.

25. Barnett, Kenneth M., "A Description of the Artillery Meteorological Comparisons at White Sands Missle Range, October 1974 - December 1974 ('PASS' - Prototype Artillery [Meteorological] Subsystem)," ECOM-5589, April 1976.
26. Miller, Walter B., "Preliminary Analysis of Fall-of-Shot From Project 'PASS'," ECOM-5590, April 1976.
27. Avara, Elton P., "Error Analysis of Minimum Information and Smith's Direct Methods for Inverting the Radiative Transfer Equation," ECOM-5591, April 1976.
28. Yee, Young P., James D. Horn, and George Alexander, "Synoptic Thermal Wind Calculations from Radiosonde Observations Over the Southwestern United States," ECOM-5592, May 1976.
29. Duncan, Louis D., and Mary Ann Seagraves, "Applications of Empirical Corrections to NOAA-4 VTPR Observations," ECOM-5593, May 1976.
30. Miers, Bruce T., and Steve Weaver, "Applications of Meterological Satellite Data to Weather Sensitive Army Operations,"ECOM-5594, May 1976.
31. Sharenow, Moses, "Redesign and Improvement of Balloon ML-566," ECOM-5595, June, 1976.
32. Hansen, Frank V., "The Depth of the Surface Boundary Layer," ECOM-5596, June 1976.
33. Pinnick, R.G., and E.B. Stenmark, "Response Calculations for a Commercial Light-Scattering Aerosol Counter," ECOM-5597, July 1976.
34. Mason, J., and G.B. Hoidale, "Visibility as an Estimator of Infrared Transmittance," ECOM-5598, July 1976.
35. Bruce, Rufus E., Louis D. Duncan, and Joseph H. Pierluissi, "Experimental Study of the Relationship Between Radiosonde Temperatures and Radiometric-Area Temperatures," ECOM-5599, August 1976.
36. Duncan, Louis D., "Stratospheric Wind Shear Computed from Satellite Thermal Sounder Measurements," ECOM-5800, September 1976.
37. Taylor, F., P. Mohan, P. Joseph and T. Pries, "An All Digital Automated Wind Measurement System," ECOM-5801, September 1976.
38. Bruce, Charles, "Development of Spectrophones for CW and Pulsed Radiation Sources," ECOM-5802, September 1976.
39. Duncan, Louis D., and Mary Ann Seagraves,"Another Method for Estimating Clear Column Radiances," ECOM-5803, October 1976.
40. Blanco, Abel J., and Larry E. Taylor, "Artillery Meteorological Analysis of Project Pass," ECOM-5804, October 1976.
41. Miller, Walter, and Bernard Engebos," A Mathematical Structure for Refinement of Sound Ranging Estimates," ECOM-5805, November, 1976.
42. Gillespie, James B., and James D. Lindberg, "A Method to Obtain Diffuse Reflectance Measurements from 1.0 to 3.0 μm Using a Cary 17I Spectrophotometer," ECOM-5806, November 1976.
43. Rubio, Roberto, and Robert O. Olsen,"A Study of the Effects of Temperature Variations on Radio Wave Absorption,"ECOM-5807, November 1976.
44. Ballard, Harold N., "Temperature Measurements in the Stratosphere from Balloon-Borne Instrument Platforms, 1968-1975," ECOM-5808, December 1976.
45. Monahan, H.H., "An Approach to the Short-Range Prediction of Early Morning Radiation Fog," ECOM-5809, January 1977.
46. Engebos, Bernard Francis, "Introduction to Multiple State Multiple Action Decision Theory and Its Relation to Mixing Structures," ECOM-5810, January 1977.
47. Low, Richard D.H.,"Effects of Cloud Particles on Remote Sensing from Space in the 10-Micrometer Infrared Region," ECOM-5811, January 1977.
48. Bonner, Robert S., and R. Newton, "Application of the AN/GVS-5 Laser Rangefinder to Cloud Base Height Measurements," ECOM-5812, February 1977.
49. Rubio, Roberto, "Lidar Detection of Subvisible Reentry Vehicle Erosive Atmospheric Material," ECOM-5813, March 1977.
50. Low, Richard D.H., and J.D. Horn, "Mesoscale Determination of Cloud-Top Height: Problems and Solutions," ECOM-5814, March 1977.

51. Duncan, Louis D., and Mary Ann Seagraves, "Evaluation of the NOAA-4 VTPR Thermal Winds for Nuclear Fallout Predictions," ECOM-5815, March 1977.
52. Randhawa, Jagir S., M. Izquierdo, Carlos McDonald and Zvi Salpeter, "Stratospheric Ozone Density as Measured by a Chemiluminescent Sensor During the Stratcom VI-A Flight," ECOM-5816, April 1977.
53. Rubio, Roberto, and Mike Izquierdo, "Measurements of Net Atmospheric Irradiance in the 0.7- to 2.8-Micrometer Infrared Region," ECOM-5817, May 1977.
54. Ballard, Harold N., Jose M. Serna, and Frank P. Hudson Consultant for Chemical Kinetics, "Calculation of Selected Atmospheric Composition Parameters for the Mid-Latitude, September Stratosphere," ECOM-5818, May 1977.
55. Mitchell, J.D., R.S. Sagar, and R.O. Olsen, "Positive Ions in the Middle Atmosphere During Sunrise Conditions," ECOM-5819, May 1977.
56. White, Kenneth O., Wendell R. Watkins, Stuart A. Schleusener, and Ronald L. Johnson, "Solid-State Laser Wavelength Identification Using a Reference Absorber," ECOM-5820, June 1977.
57. Watkins, Wendell R., and Richard G. Dixon, "Automation of Long-Path Absorption Cell Measurements," ECOM-5821, June 1977.
58. Taylor, S.E., J.M. Davis, and J.B. Mason, "Analysis of Observed Soil Skin Moisture Effects on Reflectance," ECOM-5822, June 1977.
59. Duncan, Louis D. and Mary Ann Seagraves, "Fallout Predictions Computed from Satellite Derived Winds," ECOM-5823, June 1977.
60. Snider, D.E., D.G. Murcray, F.H. Murcray, and W.J. Williams, "Investigation of High-Altitude Enhanced Infrared Backround Emissions" (U), SECRET, ECOM-5824, June 1977.
61. Dubbin, Marvin H. and Dennis Hall, "Synchronous Meteorlogical Satellite Direct Readout Ground System Digital Video Electronics," ECOM-5825, June 1977.
62. Miller, W., and B. Engebos, "A Preliminary Analysis of Two Sound Ranging Algorithms," ECOM-5826, July 1977.
63. Kennedy, Bruce W., and James K. Luers, "Ballistic Sphere Techniques for Measuring Atomspheric Parameters," ECOM-5827, July 1977.
64. Duncan, Louis D., "Zenith Angle Variation of Satellite Thermal Sounder Measurements," ECOM-5828, August 1977.
65. Hansen, Frank V., "The Critical Richardson Number," ECOM-5829, September 1977.
66. Ballard, Harold N., and Frank P. Hudson (Compilers), "Stratospheric Composition Balloon-Borne Experiment," ECOM-5830, October 1977.
67. Barr, William C., and Arnold C. Peterson, "Wind Measuring Accuracy Test of Meteorological Systems," ECOM-5831, November 1977.
68. Ethridge, G.A. and F.V. Hansen, "Atmospheric Diffusion: Similarity Theory and Empirical Derivations for Use in Boundary Layer Diffusion Problems," ECOM-5832, November 1977.
69. Low, Richard D.H., "The Internal Cloud Radiation Field and a Technique for Determining Cloud Blackness," ECOM-5833, December 1977.
70. Watkins, Wendell R., Kenneth O. White, Charles W. Bruce, Donald L. Walters, and James D. Lindberg, "Measurements Required for Prediction of High Energy Laser Transmission," ECOM-5834, December 1977.
71. Rubio, Robert, "Investigation of Abrupt Decreases in Atmospherically Backscattered Laser Energy," ECOM-5835, December 1977.

☆ U.S. GOVERNMENT PRINTING OFFICE: 1977 777-093/24